The role of charge reversal of iron ore tailing sludge on the flocculation tendency of sediments in marine environment

Grilo, C. F.; Chassagne, C.; Quaresma, V. da S.; van Kan, P. J.M.; Bastos, A. C.

DOI
10.1016/j.apgeochem.2020.104606

Publication date
2020

Document Version
Accepted author manuscript

Published in
Applied Geochemistry

Journal Pre-proof

The role of charge reversal of iron ore tailing sludge on the flocculation tendency of sediments in marine environment

C.F. Grilo, C. Chassagne, V. da S. Quaresma, P.J.M. van Kan, A.C. Bastos

PII: S0883-2927(20)30092-5

DOI: https://doi.org/10.1016/j.apgeochem.2020.104606

Reference: AG 104606

To appear in: *Applied Geochemistry*

Received Date: 21 January 2019

Revised Date: 1 April 2020

Accepted Date: 19 April 2020

Please cite this article as: Grilo, C.F., Chassagne, C., Quaresma, V.d.S., van Kan, P.J.M., Bastos, A.C., The role of charge reversal of iron ore tailing sludge on the flocculation tendency of sediments in marine environment, *Applied Geochemistry* (2020), doi: https://doi.org/10.1016/j.apgeochem.2020.104606.

THE ROLE OF CHARGE REVERSAL OF IRON ORE TAILING SLUDGE ON THE FLOCCULATION TENDENCY OF SEDIMENTS IN MARINE ENVIRONMENT

Grilo, C.F.[1*]; Chassagne, C.[2]; Quaresma, V. da S.[1]; van Kan, P.J.M.[3]; Bastos, A. C.[1]

[1]Marine Geosciences Lab (LaboGeo), Department of Oceanography and Ecology, Federal University of Espírito Santo, Vitória 29075-910, Espírito Santo, Brazil.

[2]Environmental Fluid Mechanics Lab, Geoscience & Engineering, Delft University of Technology, Mekelweg 5, 2628 CD Delft. The Netherlands.

[3]Van Kan Scientific, Keucheniuspad 40, 6535 VR Nijmegen, The Netherlands. vankanscientific@xs4all.nl

**Corresponding author: carolinegrilo@gmail.com*

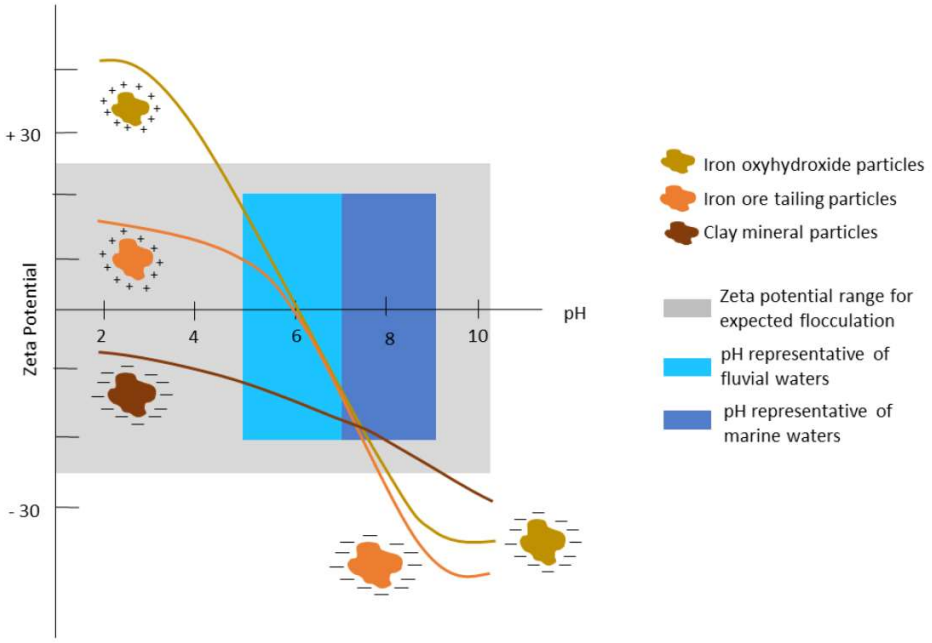

THE ROLE OF CHARGE REVERSAL OF IRON ORE TAILING SLUDGE ON THE FLOCCULATION TENDENCY OF SEDIMENTS IN MARINE ENVIRONMENT

ABSTRACT

In the mining industry, tailings are conventionally stored in artificial ponds that are susceptible to ruptures, as occurred in Southeast Brazil in November 2015. The Fundão failure dumped approximately 40 million m^3 of very fine iron-rich tailing material into the Doce River watershed, where part reached the adjacent continental shelf. Part of the spilled material remained suspended in the water column after reaching the ocean. Zeta potential measurements (pH and salt dependence) were conducted to verify the flocculation tendency of suspensions. Surface sediment samples were collected in areas representative of key stages of tailings transport through the river and subsequent deposit on the continental shelf. A surface sediment sample from the continental shelf prior to the failure was used as a control. Previously published data suggested an influence from goethite on the flocculation of samples containing iron ore tailing sludge. Here we show that although a flocculation tendency was observed under influence of salts, the presence and quantity of iron oxyhydroxide were determinant in the flocculation pattern of contaminated sedimentary samples. Only sediment from the continental shelf before the mining dam breach exhibited classical zeta potential behavior dependence on pH and salinity expected in natural sediments containing clay minerals. Sediments contaminated with the iron ore tailing sludge displayed a clear influence of goethite on their zeta potential.

Key words: flocculation, Doce River, iron ore, zeta potential, iron oxyhydroxide.

1 INTRODUCTION

tailings generated by mega-scale mining operations. In many cases, tailings are conventionally stored in artificial ponds or dams that are susceptible to accidental discharges and ruptures. A number of associated environmental issues pose significant risks to the human population in the surrounding areas (Wang et al., 2014).

In Brazil, one of the most important mining companies is Samarco Mineração S.A., that specializes in processing itabirite. Itabirite is an ore with low iron content and fine grain size, composed primarily of quartz and hematite. The quartz is undesirable and removed, leaving a residue after treatment that has approximately 57% iron content (Pires et al., 2003). This residue is a fluid of fine mineral tailings which consists of a mixture of by-products of waste generated by the recovery of minerals, metals and other ore resources that pass through a selective extraction and processing to form the tailings stream. After processing the itabirite, two products are generated by Samarco Mineração S.A.: a concentrate, which is transported via pipeline for shipment, and a tailing sludge (residue) that is deposited in dams. In the dams, the solids and process fluids separate by gravity after a long sedimentation time that promotes the formation of gels resistant to consolidation. This gel also binds a significant volume of process water (Wang et al., 2014).

In November 2015, a mining dam failure dumped approximately 40 million m^3 of very fine iron-rich tailing material into the Doce River watershed and onto the adjacent continental shelf of Southeast Brazil. Settling column experiments (Grilo et al., 2018) conducted after the mining dam breach demonstrated different properties and behavior of flocs between natural sediment samples and those contaminated by the iron ore tailing sludge. The presence of smaller and more porous flocs in the latter was explained by a very fine fraction of clay and/or a metallic coating. Santos and Brandão (2003) studied a dam at the same iron ore processing complex and showed that the extensive presence of goethite in the residue generates a fine porous material (96 % < 2 mm, with the largest

during reverse cationic flotation (Nakhaei and Irannajad, 2018), where goethite is considered to be a sludge generator and therefore is removed in desliming process followed by its deposition in the dam (Totou et al., 2011)

Nanoparticles such as iron oxyhydroxides from the dam breach may lead to serious environmental risks if they have a long residence time in the water column. Their aggregation with native components (clays, organic matter and plankton) and ingestion by organisms (plankton and nekton) and subsequent transport and deposition will have a strong biogeochemical impact (Darland and Inskeep, 1997; Ju-Nam and Lead, 2008; Lin et al., 2010; Qafoku, 2010). The nanoparticles' unique physical and chemical properties, due to their high surface area to volume ratio and nanoscale size, leads to their transport over large distances, persistence and bioavailability in the environment, all essential parameters to be considered in risk assessment and management (Wiesner et al., 2009). Changes in size due to their aggregation can also significantly alter transport potential as well as their reactivity, toxicity and bioavailability properties (Klaine et al., 2008; Xu et al., 2015). The nanoparticles that aggregate will settle and be less prone to dispersion, while the sorbent mineral will act as a sink for metal ions. Subsequently, changes in the pH and redox conditions make the sorbent mineral work as a chronic source of metal ions for the aqueous environment (Smith, 1999). Nanoparticles can also be ingested by organisms and potentially enter the food chain (Wiesner and Bottero, 2007). Assimilation and toxicity of metals in marine environments is dependent on the oxidation state of the metal and its tendency to form complexes with ligands (Domingos et al., 2015), where metal-carbonate complexes are an example of the effect of ligands on metal assimilation (Rahmana et al., 2014). A better understanding of the transport and deposition of the sorbent nanoparticles in regions near coral reefs and rhodolith banks, such as on the continental shelf near the Doce River, is therefore crucial.

their stability (Breeuwsma and Lyklema, 1973). The behavior of metals in aqueous media is very complex, as ions can undergo a series of chemical reactions and change their speciation according to the pH of the solution. This results in chemical products having a high reactivity with clay particles. The increase in the ionic concentration of metal ions in solution results in a decrease of the repulsive interactions. When in excess, these ions induce a charge reversal on the surface of the particle, (Hunter and James, 1992; Ma and Pierre, 1997; Wang et al., 2014), resulting in a stable suspension, which was observed in settling column experiments by Grilo et al. (2018). A critical review and evaluation of deposition and aggregation behavior of nanomaterials in aquatic systems under favorable and unfavorable conditions (Petosa et al., 2010) noted that conditions favoring particle-surface interactions (i.e. non-repulsive interactions) promote aggregation and may enhance density, resulting in deposition. While hematite is a dense and compact iron oxide of higher density, goethite has a hydrated and porous form that might result in lighter particles. Both goethite and hematite minerals exhibit variable charge, resulting in a greater reactivity relative to clay minerals (Antelo et al. 2005). After entering the aquatic environment, the composition of fluid fine mineral tailings will evolve with respect to the water chemistry and presence of other suspended particles. The stability of colloidal suspensions in the presence of an electrolyte solution can be described by the Derjaguin, Landau, Vervey, and Overbeek (DLVO) theory (Derjaguin and Landau, 1941; Verwey, 1947). While an attractive van der Waals force allows the particles to flocculate, the Coulombic forces between colloidal particles of same charge are repulsive. The relative strength between these forces will determine the stability of the suspension (i.e. if particles will aggregate or not). Non-DLVO forces also play an important role in the aggregation and deposition of colloidal particles. Some nanoparticles can contain hydrophilic material, functional groups or biomolecules on their surfaces that can trap significant quantities of water (Petosa et al., 2010) that may increase the mutual repulsion between

and behavior of suspensions, cohesion of aggregates, physical properties of tailings (viscosity and yield stress) as well as the consolidation and permeability of the bottom sediment. The zeta potential is a measure of the magnitude of repulsion or attraction between particles. The magnitude of the zeta potential is an important criterion in determining the stability of colloidal systems of charged particles. The isoelectric point (IEP) and the point of zero charge (PZC) correspond to the pH of a suspension in which amphoteric particles have a neutral charge. While the IEP determines the charge of the outer surface of the particles in solution, i.e. the pH value at which particles are electrokinetically uncharged (Everett, 1972), the PZC represents the total value, i.e. the charge of both the inner and outer surfaces (Menéndez et al., 1995). The IEP is defined by electrokinetic measurements (Kosmulski, 2016) and corresponds to the charge at the plane of shear. Thus, the pH corresponding to the IEP also corresponds to the PZC, where the particle has no charge. The PZC can also be reached by addition of salt. In that case, there is no IEP (i.e. the surface of the particle remains charged), but the concentration of counterions behind the plane of shear is such that they compensate for the surface charge. At the PZC, the particle appears uncharged even though it is charged, the zeta potential is zero, and the suspension unstable, as particles can then easily flocculate and consequently settle. The PZC can be reached either by adjusting the ionic strength of the suspension, in which case the surface charge of the particle is (for a given ionic strength) fully screened by counterions from the added electrolyte, or by adjusting the pH, in which case the surface charge of the particle is modified so as to carry no net charge (for a given pH). From DLVO theory, it can be estimated that the flocculation occurs for zeta potential values between +25 and -25 mV (Hunter et al., 1981). If particles are anisotropic with different surface charge groups and non-DLVO forces can play a role, these boundary values of +25 and -25 mV are subject to change and should be used with caution (Chassagne et al., 2009).

delayed flocculation (Grilo et al., 2018). The focus of this work is to explore and define how the electrochemical properties of particles coming from the mining breach may be influencing the delayed flocculation and settlement of material exported by the Doce River after the iron ore dam breach. The marine area adjacent to the river mouth is known as favorable to flocculation. A depocenter was already documented (Quaresma et al., 2015). The data presented here reinforce the influence of the tailing sludge on the behavior of fine material when it enters the marine environment.

Zeta potential measurements were conducted to verify 1) if iron ore tailing sludge is promoting delayed flocculation due to the great abundance of iron oxyhydroxide in the composition; 2) if delayed flocculation is dependent on salts and/or pH differences between the fluvial Doce River environment and marine waters; and 3) if the new particles coming from the iron ore tailing sludge aggregate with the natural sediment. The measurements were performed by varying pH and using multiple electrolyte solutions at several ionic strengths. The pH and salinities used are representative of environments in which the spilled material can be found along the Doce River and adjacent continental shelf. Zeta potential analysis was also performed with pure synthetic goethite (PS goethite) suspensions to serve as an iron oxyhydroxide reference due to the great abundance of goethite in the iron ore tailing sludge (Santos and Brandão, 2003; Pires et al., 2003; Quast, 2012;). A sample from the continental shelf prior to the mining dam failure was used for comparison purposes as a control.

2 MATERIALS AND METHODS

2.1 Sampling and background information

analysis. Sampling sites are presented in Figure 1; their respective particle size distributions for the mud fraction (< 63µm) of bottom sediment samples are presented in Figure 2 (further detail in Grilo et al., 2018).

The Mining Dam (MD) sample is considered to be representative of the iron ore tailing sludge end-member, while the Continental Shelf 1 (CS 1; before dam breach) represents the end-member without the iron ore tailing sludge input (sampled before the dam breach). The Doce River bed sediment sample (RV) represents the mixture between the iron ore tailing sludge and riverbed sediment prior to the rupture of the dam before entering the marine environment; sampling occurred after the iron ore tailing sludge input. The influence of the dam breach on the continental shelf sediment is represented by the differences between CS 1 and Continental Shelf 2 (CS 2; after the breach), where the latter contains a mixture of sediment (and tailing sludge) exported by the Doce River before and after the mining dam breach. Flocculation tendency of these same samples in settling column experiments are also presented in Grilo et al. (2018), where authors identified minor flocs and slower settling velocity for RV sample.

The historical average of pH for the Doce River is ≈ 7, but during the “mud tide” (mix of mud and iron tailing sludge transported downstream) was variable; at some points it reached values near 6 (Instituto Mineiro de Gestão de Águas, 2016). pH values from an ongoing monitoring has registered an average of 7.39 ± 0.34 for fluvial waters before reaching estuarine area and an average of 7.44 ± 0.38 at the estuary mouth (Fundação Renova, 2019). pH values for coastal waters at adjacent continental shelf usually range between 7.5-8.45 (MMA, 2006) and presented an average of 8.48 ± 0.19 in a monitoring during December 2015 (Golder, 2017). Marine water has not been observed in proximity to the RV sediment sample site; its salinity is of fluvial water (0.25 ± 0.32; Fundação Renova, 2019). Mineralogical analysis of the sediment indicates the presence of goethite, kaolinite,

PS (Pure Synthetic) goethite was prepared based on Villacís-García et al. (2015). Briefly, a 0.5 M solution of Iron (III) nitrate nonahydrate ($(Fe(NO_3)_3 \cdot 9H_2O)$) in water was prepared. To this solution, 2M KOH was added at a rate of 10 ml/min until the pH reached 12. The precipitated slurry was aged for 60 hours in an oven at 60°C. The slurry changed color from orange-brown to ochre during ageing. The precipitate was washed with demi-water and filtered through a 0.45 µm Millipore filter for PS goethite recovery. A stock PS goethite nanoparticle suspension was prepared by diluting PS goethite with demi-water (pH 6.5). All suspensions (PS goethite and sediment samples) were sonicated for 5 min prior to measurement. All chemicals used in experiment were high-quality grade from Sigma-Aldrich.

2.3. Zeta potential measurements

The electrophoretic mobility of the suspensions was measured by Doppler velocimetry using a Zetasizer Nano ZS (Malvern Panalytical). Three different samples and over 10 subruns for each sample were performed which led to an average deviation of ± 3 mV. Complementary zeta potential measurements as a function of time were done by electrophoresis, using video microscopy (Zetameter ZetaCompact, CAD Instruments). The zeta potential values were acquired in suspensions at 9 different pH values (ranging from 2 to 10), adjusted by adding acid (HCl) or base (NaOH) and with monovalent (NaCl and KCl) and divalent ($MgCl_2$ and $CaCl_2$) salts. The pH was measured using pH indicator paper (pH range 0-14, non-bleeding; Whatman), having an accuracy within one pH value. Electrolyte solutions were prepared with demi-water (conductivity < 10 μS/cm; pH 6). A dilution of the bulk sediment of each sample was made until the desired sediment concentration was achieved. Directly afterwards, samples were injected into the cell for measurements of the electrophoretic mobility of the suspensions. The voltage applied during measurements was 50 V, an optimal value for these types of measurements as established by Chassagne and Ibanez (2013). The temperature was

201 The electrophoretic mobility values are given as 'apparent' zeta potential (AZP) values (mV) using the
202 Smoluchowski formula: $\zeta = \eta u/\varepsilon$, where u is electrophoretic mobility of the particle, η is the viscosity
203 of the suspending liquid, ε is the dielectric constant of the suspending medium, and ζ is the zeta
204 potential (Hunter 1981). In line with Kaya et al. (2006), we used +25 and -25 mV limits (gray areas in
205 Figures 3, 4, 5 and 6) to indicate the flocculation range. It is expected that aggregates can be
206 approximated by spheres reasonably well, therefore these limits are representative for our systems.
207 As discussed above, these limits have to be adapted if the particles are anisotropic, which is the case
208 for non-flocculated goethite particles (rods). Connection lines on Figures 3 to 7 are trend lines, rather
209 than correspondent to a fitted model.

210 Measurements on the interaction between kaolinite and PS goethite were also performed to verify
211 the flocculation tendencies between these two types of particles. The PS goethite and kaolinite were
212 mixed the day before the analysis to allow sufficient time for the particles to interact and stabilize.
213 The kaolinite (China clay $Al_2O_3—2SiO_2—2H_2O$) was obtained from VE-KA Industrie Keramische
214 Grondstoffen Ltd., The Netherlands. Goethite was synthesized as described below.

215

216 **3 RESULTS**

217 AZP dependence on pH (2 to 10; Figure 3) and monovalent (KCl and NaCl; Figure 4) and divalent
218 ($MgCl_2$ and $CaCl_2$; Figure 5) salts assessed the surface charge of suspended particles in aqueous
219 solution to better understand the flocculation of studied samples and PS goethite in different
220 electrolytes. An addition of PS goethite to the CS 1 sample (obtained prior to the failure) and to the
221 kaolinite sample were also analyzed to define the influence of goethite on natural sediments (Figure
222 6). Kaolinite was chosen due to its great abundance in the Doce River sedimentary basin. It is a
223 characteristic mineral in sediments resulting from the weathering of feldspars in the quartz-rich

226 3.1 Zeta potential dependence on pH

227 Although sediment samples were collected in different environments (mining pond, fluvial and
228 marine waters), those containing the iron ore tailing sludge (MD, RV and CS 2) presented the same
229 pattern under a varying pH, where a charge reversal (PS goethite and MD sample) and a sudden jump
230 (CS 2 and RV samples) in the AZP values occurred in the same pH range (between 6 and 7; Figure 3).
231 PS goethite AZP values were nearly constant for acidic (positive AZP) and basic (negative AZP) pHs.
232 The sediment from the continental shelf prior to the failure exhibited a continuous and gradual
233 increase of negative charge with increasing pH, without any jump or charge reversal.

234 3.2 Zeta potential dependence on monovalent and divalent salts

235 AZP values of sediment samples and PS goethite for monovalent (NaCl and KCl) and divalent ($MgCl_2$
236 and $CaCl_2$) salts are presented in Figures 4 and 5. The sediment samples exhibited similar trends with
237 increasing electrolyte concentration, mainly for divalent salts. The sample most sensitive to salt
238 influence was MD while RV was the least sensitive for monovalent salt, with initial AZP values near -
239 40 mV and reaching a value of -22.9 mV at 30 mM KCl. For divalent salts, CS 1 was slightly less
240 sensitive than the others. AZP trends for continental shelf samples were very similar, although CS 1
241 exhibited lower AZP values for monovalent salts than CS 2. For PS goethite, divalent salts had a
242 stronger influence on the AZP values than monovalent salts.

243

244 **4 DISCUSSION**

245 Iron oxyhydroxide particles are usually found in very small sizes (a few micrometers to a few
246 nanometers), resulting in a high surface-to-volume ratio and a high reactivity to changes in
247 environmental conditions. Reactions at the solution/iron oxyhydroxide interface influence oxide

containing particles, where type, concentration and pH of the electrolyte strongly affect aggregates' properties (Baalousha, 2009).

From Figure 3, we conclude that sediments samples (CS 1, CS 2, RV and MD) are prone to flocculate at pH ≤ 6 and deflocculate at pH ≥ 7. As for PS goethite, flocculation may occur only in a very narrow pH range, between pH 6 and 7, when a charge reversal occurs. This charge reversal has shown to be an interesting feature to track iron oxyhydroxide in the sediment samples, as it is also a feature for goethite-rich sediment samples (as seen in MD data in Figure 3). The difference between CS 1 and CS 2 (before/after the dam failure) clearly shows the impact of goethite on the AZP behavior. Although, charge reversal for the CS 2 and RV samples does not occur as for the MD sample, the decline trend is comparable to the charge reversal in the same range as for PS goethite. The reversal absence can be explained by the mixing of riverine and marine sediment and the amount of iron oxyhydroxide.

Typical charge curves of metal oxides present an amphoteric behavior (Koopal, 1996). Because goethite is a hydrated form of metal oxide (oxyhydroxide metal) it also exhibits a classical behavior of charge variation just like minerals that have pH dependence (Livage et al., 1988; Xu et al., 2015), having an almost constant AZP for acidic (positive AZP) and basic (negative AZP) pH values. Outside the reversal zone (6 – 7 pH), the suspension is stable and does not tend to flocculate. An essential characteristic for the formation and development of charges in variable charge colloids is the possibility of hydroxylation at their surfaces. In the presence of water, iron ions located on the surface of minerals such as goethite complete their coordination layer with a water molecule, thus the entire surface becomes hydroxylated (Stumm, 1992).

The influence of organic matter (polyelectrolytes) present in the RV and CS samples on the charge reversal of goethite was not studied, but Figure 3 seems to indicate that their presence does not influence the position (between pH = 6-7) of the reversal, as it occurs in the same range for RV, MD

during the transport downstream in the Doce River resulted in differences in composition and particle sizes between these two samples. Complexation of metals by dissolved ligands may increase or inhibit sorption reactions (Davis and Leckie, 1978), in which complexation with inorganic ligands (Smith, 1999) and humic acid (Chekli et al., 2013) tends to inhibition. Although iron nanoparticles enveloped by humic acid have a higher stability under pH changes (Chekli et al., 2013), the charge reversal for sediment samples is in the same range as for PS goethite; the electrical double layer compression under high concentration of NaCl and the similar response of the electrical double layer compression by $CaCl_2$ and $MgCl_2$ exclude this envelopment hypothesis.

In aqueous media, considering a system with no organic and inorganic ligands, the ferric ions of a oxyhydroxide particle coordinate with OH^- groups (hydroxyl) or water molecules by sharing a free electron pair of the oxygen atom with iron. During adsorption, the water molecules usually dissociate and cover the ferric ions with OH^- groups (Livage et al., 1988). This hydroxylation reaction is fast and is followed by the binding of other water molecules through hydrogen bonds to OH^- groups (active and on the surface of the particle). The bound OH^- group still has a double pair of electrons and a dissociable proton that allows its reaction with acids and bases (Livage et al., 1988; Smith, 1999; Fontes et al., 2001; Cornell and Schwertmann, 2003). In this way, charge reversal (positive in acid pH and negative in basic pH) of PS goethite is a result of gradual protonation/deprotonation with decreasing/increasing pH and repulsive forces overcame van der Waals force when the suspension pH is ≤ 6/≥ 7 (Xu et al.,2015).

Kaolinite is a clay mineral and its surface charge is also pH-dependent (Gupta and Miller, 2010; Yan et al., 2011), although it is less sensitive to deprotonation with increasing pH than metal oxides (Wang et al., 2014). The PZC of alumina faces of the kaolinite is between 6 and 8 (Gupta and Miller, 2010), implying that only at pH > 8 the kaolinite discs are fully charged (Zhou and Gunter, 1992). CS 1

300 without tailing sludge input and was the only one to behave in a similarly way to a natural clay
301 mineral, having a permanent negative charge (Smith, 1999; Fontes et al., 2001) when no other
302 ligands (organic matter and dissolved metals) are considered. Samples presenting both clay particles
303 and tailing sludge (MD, RV and CS 2 sediment) have a different behavior, as if the final AZP of the
304 sample was the sum of the values of oxyhydroxide and clay minerals particles. That means under acid
305 pH, the greater the amount of oxyhydroxide the more AZP will tend to positive values, while under
306 basic pH the AZP will tend to negative values, as the PS goethite curve showed positive and negative
307 AZP values for acidic and basic pH, respectively; the quantity of iron oxyhydroxide is shown to be
308 determinant for the flocculation and settling processes.

309 Besides hydroxylation, the compression of the electrical double layer for sediment samples under the
310 influence of salts lead to an increase of the AZP with the increase of electrolyte concentration
311 (Figures 4 and 5), which is typical for indifferent ions (Smith, 1999; Kosmulski, 2002), where divalent
312 salts impose greater double layer compression than monovalent salts (Ibanez et al., 2014),
313 particularly for MD sample. In presence of monovalent salts (KCl and NaCl) no flocculation is
314 expected based on the values of the AZP (> 25 mV), while in the presence of divalent cationic salts
315 ($MgCl_2$ and $CaCl_2$) flocculation is expected, even at a low salt concentration (1 mM). As seawater
316 contains a substantial quantity of divalent cations (for a salinity of 35, approximately 300 times more
317 dissolved salts than average river water; about 545, 52 and 10 milimol/kg respectively for Cl^-, Mg^{2+}
318 and Ca^2+; Pilson, 1998; Millero, 2006) flocculation is therefore expected in the transition zone
319 between the river and the continental shelf. The AZP of PS goethite is almost constant with salt
320 addition. The AZP decreases for high salinities; the surface charge is then screened to such an extent
321 that mobility is affected.

322 From the results it can be determined that pH variation is more important for flocculation in

(see CS 1), are negatively charged. This implies that below pH = 6, strong flocculation is expected between goethite and clay particles, but for pH > 7 these particles tend to repel. A discussion about interaction between goethite and clay particles is written below.

4.1 Binding of goethite to sediment

Even though the influence of iron oxyhydroxide is clearly visible on the AZP, it remains to be investigated if the goethite is simply mixed with the sediment, or if it is (partially) bound to it. As we know that the sediment of the Doce River is in large part composed of kaolinite, we used this clay mineral as a proxy for the RV before disaster. According to Zhou and Gunter (1992), at high pH (pH ≥ 8) all kaolinite surfaces become negatively charged, kaolinite particles are dispersed and the suspension is stable. As PS goethite presented a high negative AZP at basic pH (pH ≥ 7), it will not (easily) aggregate with kaolinite. As stated in the introduction, salt-induced aggregation is possible thanks to van der Waals forces at high ionic strength, so flocculation between PS goethite and kaolinite is expected at high ionic strength (such as in seawater). However, salt-induced flocs are extremely sensitive to shear (Chassagne et al., 2009), so the flocs are not likely to grow large in energetically active regions like the adjacent continental shelf to the Doce River mouth. A detailed study on the interaction between PS goethite and kaolinite particles was therefore made at acidic pH, where flocculation would be easily possible due to opposite charges. The flocs obtained are also stronger, as the PZC would correspond to the IEP, implying that the flocs will aggregate in the region of interaction energy corresponding to the primary minimum (Hunter et al., 1981).

A change in the suspension AZP in relation to PS goethite addition was found, when different proportions of PS goethite were added to suspensions of pure kaolinite (Figure 6). The bottom panel of Figure 6 shows that kaolinite might indeed react with PS goethite as the dependence on PS goethite is not linear. The CS 1 sample exhibits a linear dependence on the addition of PS goethite

350 contains other minerals including those coming from the Doce River watershed (like muscovite,
351 gibbsite and illite; Tintelnot et al., 1998) and those produced *in situ* (carbonates; Quaresma et al.,
352 2015).

353 To confirm the interaction between goethite particles and kaolinite, additional electrophoretic
354 mobility experiments were performed using video microscopy (Figure 7). It takes approximately 15
355 min to reach an equilibrium AZP distribution in that case. The goethite-kaolinite interaction is thus
356 not fast, considering the fact that they are oppositely charged, but one should remember that the
357 edges of kaolinite become positive at pH < 5 (Williams and Williams, 1978; as in the present
358 experiment) due to exposed hydroxyl groups coming from Si-OH and Al-OH situated at the broken
359 edges (Tombácz and Szekeres, 2006) and may result in a weak repulsion from the edge side. Even
360 with edges presenting positive charge under low pH, the negative and permanent charge of the basal
361 plane controls the overall electrokinetic behavior of the clays (Preocanin et al., 2016). In marine
362 environment the repulsion between goethite and kaolinite particles may become even greater, as
363 goethite turns negative in basic conditions. This will result in different transport mechanisms for
364 tailing sludge versus the natural sediment. During the mining dam failure event, two plumes were
365 identified in the marine environment: one with a wider dispersion at the surface (probably mostly
366 composed of iron oxyhydroxide nanoparticles) and another of a high-concentrated suspended
367 particulate matter plume near the bottom (probably most composed of kaolinite-rich sediment)
368 (Directorate of Hydrography and Navigation of Brazil, 2015).

369 Reactions on the surface of a crystalline solid such as goethite are difficult to describe due to the
370 multiple functional groups that have different protonation and deprotonation trends. When the
371 binding occurs with carbonic acid (H_2CO_3), the surface of the goethite becomes positive; when the
372 bond is made with bicarbonate (HCO_3^-), the surface becomes negative (van Geen et al., 1994). This is

375 samples, the only one to not present a surface charge reversal or a sudden jump in AZP was CS 1,
376 indicating a deprotonation pattern in all others.

377 The change of flocculation tendency between circumneutral do basic conditions is of fundamental
378 importance for the knowledge of the dispersion pattern of suspended particles exported by the river,
379 as it corresponds to a transition from fluvial to marine environments. Fluvial waters generally vary in
380 pH between 5 and 7 (≈ 7 for the Doce River; Instituto Mineiro de Gestão de Águas, 2016) while
381 typical marine waters have an average pH = 8.1 (NOAA, 2019), reaching a minimum of 7.5 at the
382 adjacent continental shelf (MMA, 2006) mainly because fluvial water input. As the AZP values of
383 sediment samples indicate that they are prone to flocculation at pH < 7, suspensions were unstable
384 and particles tended to settle inside the river. As soon as sediment reached coastal waters through
385 the transport of fluvial flux toward the ocean, the pH reach values higher than 7 dues to the mixing
386 of fluvial and marine waters. The suspension turns stable as they leave the flocculation range limits.

387 Such delayed-flocculation behavior for the samples implies that sediment exported by the river after
388 the mining dam breach is more prone to be dispersed in the marine environment. Sediment before
389 the failure (CS 1) can be considered naturally weathered, containing clay minerals and exhibiting
390 flocculation upon reaching the shelf. As much of the tailing sludge was deposited on the side banks
391 and floodplains along the Doce River (Carmo et al., 2017 and references therein) and although iron
392 hydroxides are found unstable in the fluvial environment (as indicated by the AZP), flood events may
393 erode and transport these particles to the marine environment, where they will undergo a
394 desorption process and release metals that were previously adsorbed (Pires et al., 2003; Hatje et al.,
395 2017; Queiroz et al., 2018). As the river conditions recover and the pH returns from acidic values to
396 circumneutral/moderately alkaline values, some metals may desorb from solid phases such as iron
397 oxyhydroxides due to cationic competition (Olías et al. 2004) and became free in the water column to

399 continuous source of metals to the aquatic environment and may become a permanent source of
400 contamination.

401

402 **5 CONCLUSION**

403 The apparent zeta potential analysis allowed us to make inferences regarding the flocculation
404 tendency for sediments contaminated with iron ore tailing sludge and PS goethite under the
405 influence of varying pH (2 to 10) and ionic strength of monovalent (NaCl and KCl) and divalent ($MgCl_2$
406 and $CaCl_2$) salts. Even though contaminated samples with tailings presented flocculation tendency
407 under influence of divalent salts, the presence (and amount) of iron oxyhydroxides and their charge
408 dependence on pH variation were determinant in the flocculation pattern of sedimentary samples.
409 When sediments were also subjected to pH variation, the iron oxyhydroxide signal could be clearly
410 tracked in other environmental matrices containing the iron ore tailing sludge, such as sediment
411 samples from inside the mining dam, inside the Doce River main channel and from the continental
412 shelf adjacent to the Doce River mouth in samples collected after the mining dam breach. While the
413 sediment for the continental shelf before the input of the iron ore tailing material are typical natural
414 weathered sediments containing clay minerals, sediments contaminated with the iron ore tailing
415 sludge had a clear influence of iron oxyhydroxide on their apparent zeta potential pattern. This has
416 great implications for the transport and deposition of this new sediment (mixture of clay minerals
417 and iron ore tailing sludge) on the continental shelf, as it is more prone to be dispersed in marine
418 environments due to a charge reversal of goethite when the pH turns basic.

419 The present study was conducted under hydrochemical conditions (pH and dissolved salts) that are
420 common in natural environments. The results can thus be used for predicting the transport and
421 deposition of iron oxyhydroxide nanoparticles as well as sediments contaminated by iron ore tailing

6 ACKNOWLEDGMENTS

This work was supported by the Science and Technology Bureau of Espírito Santo State (FAPES; grant numbers 0661/2015 and 77683390/17). The authors also thank the Coordination for the Improvement of Higher Education Personnel (CAPES), the Department of Ecology and Oceanography (DOC), the Post-Graduate Program in Environmental Oceanography (PPGOAM) of the Federal University of Espírito Santo (UFES), Miguel Lucas del Pardo and the Deltares Research Institute (The Netherlands).

7 REFERENCES

Antelo, J., Avena, M., Fiol, S., López, R. & Arce, F. 2005. Effects of pH and ionic strength on the adsorption of phosphate and arsenate at the goethite-water interface. J. Colloid Interf. Sci. 285 (2), 476–486.

Baalousha, M. 2009. Aggregation and disaggregation of iron oxide nanoparticles: influence of particle concentration, pH and natural organic matter. Sci. Total Environ. 407, 2093–2101.

Breeuwsma, A., Lyklema, J. 1973. Physical and chemical adsorption of ions in the electrical double layer on hematite (a-Fe2O3). J. Colloid Interf. Sci. 43,437–448.

Carmo, F.F., Kamino, L.H.Y., Junior, R.T., de Campos, I.C., do Carmo, F.F., Silvino, G., de Castro, Kenedy J. da S.X., Mauro, M.L., Rodrigues, N.U.A., Miranda, M.P. de S., Pinto, C.E.F. 2017. Fundão tailings dam failures: the environment tragedy of the largest technological disaster of Brazilian mining in global context. PECON. 15 (3), 145-151.

Chassagne, C., Mietta, F., Winterwerp, J. C. 2009. Electrokinetic study of kaolinite suspensions. J. Colloid Interf. Sci. 336, 352–359.

448 Chekli, L., Phuntsho, S., Roy, M., Lombi, E., Donner, E., Shon, H.K. 2013. Assessing the aggregation
449 behaviour of iron oxide nanoparticles under relevant environmental conditions using a multi-method
450 approach. Water Res. 47, 4585-4599.

451 Cornell, P.M., Schwertmann, U. 2003., The Iron Oxides: Structure, Properties, Reactions, Occurrence
452 and Uses, second ed. Wiley-VCH, Weinheim.

453 Darland, J.E., Inskeep, W.P. 1997. Effects of pH and phosphate competition on the transport of
454 arsenate. J. Environ. Qual. 26, 1133–1139.

455 Davis, J.A., Leckie, J.O. 1978. Effect of adsorbed complexing ligands on trace metal uptake by hydrous
456 oxides. Environ. Sci. Technol. 12, 1309–1315.

457 Derjaguin, B.V.; Landau, L.D. 1941. Theory of stability of strongly charged lyophobic sols and the
458 adhesion of strongly charged particles in solutions of electrolytes. Acta Phys-Chim. 14, 633–662.

459 Directorate of Hydrography and Navigation of Brazil. 2015. Levantamento ambiental expedito em
460 Regência/ES (LH-035/15): Relatório final. Technical report.

461 Domingos, R.F., Gélabert, A., Cordeiro, S.C.A., Sivry, Y., Benedetti, M.F. 2015. Metals in the Aquatic
462 Environment—Interactions and Implications for the Speciation and Bioavailability: A Critical
463 Overview. Aquat. Geochem. 21, 231–257.

464 Everett, D. H. 1972. Manual of symbols and terminology for physicochemical quantities and units.
465 Pure Appl. Chem. 31: 578-638.

466 Fontes, M.P.F., de Camargo, O.A., Sposito, G. 2001. Eletroquímica das partículas coloidais e sua
467 relação com a mineralogia de solos altamente intemperizados. Sci. Agr. 58 (3), 627-646.

468 Fundação Renova. 2019. Programa de Monitoramento Quali-Quantitativo Sistemático de Água e
469 Sedimentos – PMQQS – Maio/2019. Technical report.

472 Grilo, C. F., Quaresma, V. da S. Amorim, G. F. L., Bastos, A. C. 2018. Changes in flocculation patterns
473 of cohesive sediments after an iron ore mining dam failure. Mar. Geol. 400, 1-11.

474 Grupo da Força-Tarefa. 2016. Avaliação dos efeitos e desdobramentos do rompimento da Barragem
475 de Fundão em Mariana-MG. Technical report.

476 Gupta, V., Miller, J.D. 2010. Surface force measurements at the basal planes of ordered kaolinite
477 particles. J. Colloid Interface Sci. 344, 362–371.

478 Hatje, V., Pedreira, R.M.A., de Rezende, C.E., Schettini, C.A.F., de Souza, G.C., Marin, D.C.,
479 Hackspacher, P.C. 2017. The environmental impacts of one of the largest tailing dam failures
480 worldwide. Sci. Rep. 7 (10706), 1-13.

481 Hunter, R.J., Ottewill, R.H., and Rowell, R.L. 1981., Zeta Potential in Colloid Science: Principles and
482 Applications, first ed. Elsevier, Amsterdam.

483 Hunter, R.J., James, M. 1992., charge reversal of kaolinite by hydrolyzable metal ions: An
484 electroacoustic study. Clays Clay Miner. 40 (6), 644-649.

485 Ibanez, M., Wijdeveld, A., Chassagne, C. 2014. The role of mono- and divalent ions in the stability of
486 kaolinite suspensions and fine tailings. Clays Clay Miner. 62 (5), 374–385.

487 Instituto Mineiro de Gestão de Águas. 2016. Monitoramento da qualidade das águas superficiais do
488 Rio Doce no estado de Minas Gerais. Tecnical report.

489 Ju-Nam, Y., Lead, J.R. 2008. Manufactured nanoparticles: an overview of their chemistry, interactions
490 and potential environmental implications. Sci. Total. Environ. 400, 396–414.

491 Kaya, A., Ören, A.H., Yükselen, Y. 2006. Settling of kaolinite in different aqueous environment. Mar.
492 Georesour. Geotec. 24, 203-218.

496 Koopal L. Mineral hydroxides: from homogeneous to heterogeneous modelling. 1996. Electrochim.
497 Acta. 41, 2293–306.

498 Kosmulski, M. 2002. The pH-Dependent Surface Charging and the Points of Zero Charge. J. Colloid
499 Interf. Sci. 253, 77–87.

500 Kosmulski, M. 2016. Isoelectric points and points of zero charge of metal (hydr)oxides: 50 years after
501 Parks' review. Adv. Colloid Interfac. 238, 1–61.

502 Lin, D., Tian, X., Wu, F., Xing, B. 2010. Fate and transport of engineered nanomaterials in the
503 environment. J. Environ. Qual. 39, 1896–1908.

504 Livage, J., Henry, M., Sanchez, C. 1988. Sol-gel chemistry of transition metal oxides. Prog. Solid State
505 Ch. 18, 259-341.

506 Ma, K., Pierre, A.C. 1997. Effect of interaction between clay particles and Fe^{3+} ions on colloidal
507 properties of kaolinite suspensions. Clays Clay Miner. 45 (5), 733-744.

508 Menéndez, J.A., Illán-Gómez, M.J., Leon Y Leon, C.A., Radovic, L.R. 1995. On the difference between
509 the isoelectric point and the point of zero charge of carbons. Carbon. 33 (11): 1655-1659.

510 Millero, F.J. 2006. Chemical Oceanography, third ed. CRC Press, Boca Raton. Chapter 2.

511 Olías, M., Nieto, J.M., Sarmiento, A.M., Cerón, J.C., Cánovas, C.R. 2004. Seasonal water quality
512 variations in a river affected by acid mine drainage: the Odiel River (South West Spain). Sci. Total
513 Environ. 333, 267–281.

514 Peschel, G., Belouschek, P., Müller, M.M., Müller, M.R., König, R. 1982. The interaction of solid
515 surfaces in aqueous systems. Colloid Polym. Sci. 260, 444-451.

516 Petosa, A.R., Jaisi, D.P., Quevedo, I.R., Elimelech, M., Tufenkji, N. 2010. Aggregation and deposition of

519 Pilson, M.E.Q. 1998. An Introduction to the Chemistry of the Sea, second ed. Cambridge University
520 Press, New York. Chapter 4.

521 Pires, J.M.M., Lena, J.C., Machado, C.C., Pereira, S.P. 2003. Potencial poluidor de resíduo sólido da
522 Samarco Mineração: estudo de caso da barragem de Germano. Rev. Arvore. 27 (3), 1-8.

523 Preocanin, T., Abdelmonem, A., Montavon, G., Luetzenkirchen, J. 2016. Clays, Clay Minerals and
524 Ceramic Materials Based on Clay Minerals. IntechOpen. Chapter 3.

525 Qafoku, N.P. 2010. Terrestrial nanoparticles and their controls on soil-/geo-processes and reactions.
526 Adv. Agron. 107, 33–91.

527 Quaresma, V.S., Catabriga, G., Bourguignon, S.N., Godinho, E., Bastos, A.C. 2015. Modern
528 sedimentary processes along the Doce river adjacent continental shelf. Braz. J. Geol. 45 (4), 635–644.

529 Quast, K. 2012. Influence of 25% goethite on the surface chemistry of hematite. Int. J. Miner.
530 Process. 1 (2), 62-68.

531 Queiroz, H.M., Nóbrega, G.N., Ferreira, T.O., Almeida, L.S., Romero, T.B., Santaella, S.T., Bernardino,
532 A.F., Otero, X.L. 2018. The Samarco mine tailing disaster: A possible time-bomb for heavy metals
533 contamination? Sci. Total Environ. 637–638, 498–506.

534 Rahmana, M.A., Hogan, B., Duncan, E., Doyle, C., Krassoi, R., Rahman, M.M., Naidu, R., Lim, R.P.,
535 Maher, W., Hassler, C. 2014. Toxicity of arsenic species to three freshwater organisms and
536 biotransformation of inorganic arsenic by freshwater phytoplankton (*Chlorell*a sp. CE-35). Ecotox.
537 Environ. Safe. 106, 126-135.

538 MMA – Ministério do Meio Ambiente. 2006. Programa REVIZEE: Avaliação do potencial sustentável
539 de recursos vivos na zona econômica exclusiva. Relatório executivo. Brasília, DF: MMA, Secretaria de
540 Qualidade Ambiental, 2006. 280 p.

543 Smith, K.S. 1999. Metal sorption on mineral surfaces: An overview with examples relating to mineral
544 deposits. Rev. Econ. Geol. 6A, 161 – 182.

545 Stumm, W., 1992., Chemistry of the solid-water interface, first ed. John Wiley & Sons, New York.

546 Tombácz, E., Szekeres, M. 2006. Surface charge heterogeneity of kaolinite in aqueous suspension in
547 comparison with montmorillonite. Appl. Clay Sci. 34, 105-124.

548 Tintelnot, M., Brichta, A., Morais, J.O. 1998. Clay mineralogy of river sediments on the Brazilian coast.
549 Deutsch Geol. Ges. 1, 112-123.

550 van Geen, A., Robertson, A.P., Leckie, J.O. 1994. Complexation of carbonate species at the goethite
551 surface: Implications for adsorption of metal ions in natural waters. Geochim. Cosmochim. Ac. 58 (9),
552 2073-2086.

553 Verwey, E.J.W. 1947. Theory of the Stability of Lyophobic Colloids. J. Phys. Chem. 51 (3), 631–636.

554 Villacís-García, M., Ugalde-Arzate, M., Vaca-Escobar, K., Villalobos, M., Zanella, R., Martínez-Villegas,
555 N. 2015. Laboratory synthesis of goethite and ferrihydrite of controlled particle sizes. Bol. Soc. Geol.
556 Mex. 67 (3), 433-446.

557 Xu, C., Deng, K., Li, J., Xu, R. 2015. Impact of environmental conditions on aggregation kinetics of
558 hematite and goethite nanoparticles. J. Nanopart. Res. 17 (394), 1-13.

559 Yan, L., Englert, A.H., Masliyah, J.H., Xu, Z. 2011. Determination of Anisotropic Surface Characteristics
560 of Different Phyllosilicates by Direct Force Measurements. Langmuir. 27, 12996–13007.

561 Wang, C., Harbottle, D., Liu, Q., Xu, Z. 2014. Current State of Fine Mineral Tailings Treatment: A
562 Critical Review on Theory and Practice. Miner. Eng. 58, 113-131.

563 Wiesner, M.R., Bottero, J.-Y. 2007. Environmental Nanotechnology: Applications and Impacts of

565 Williams, D.J.A., Williams, K.P. 1978. Electrophoresis and Zeta Potential of Kaolinite. J. Colloid. Interf.
566 Sci. 65 (1), 79-87.

567 Wentwoth, C.K. 1922. A Scale of Grade and Class Terms for Clastic Sediments. J. Geol. 30 (5), 377-
568 392.

569 Wiesner, M.R., Lowry, G.V., Jones, K.L., Hochella, M.F. Jr., Di Giulio, R.T., Casman, E., Bernhardt, E.S.
570 2009. Decreasing uncertainties in assessing environmental exposure, risk, and ecological implications
571 of nanomaterials. Environ. Sci. Technol. 43 (17), 6458–6462.

572 Zhou, Z. Gunter, W.D. 1992. The nature of the surface charge of kaolinite. Clays Clay Miner. 40, 365-
573 368.

574

575 **Figure 1.** Sampling map of the study area. Red dots are sample sites: CS 1=Continental Shelf before
576 the mining dam failure; CS 2=Continental Shelf after the failure; RV=River; MD=Mining Dam. Note
577 that CS 1 and CS 2 dots overlap. Salinity and pH are indicated in the figure.

578 **Figure 2.** Particle size distribution according to Wentworth (1922) classification for the mud fraction
579 (< 63 µm) of each sample (Modified from Grilo et al., 2018). CS 1=Continental Shelf before the mining
580 dam failure; CS 2=Continental Shelf after the failure; RV=River; MD=Mining Dam.

581 **Figure 3.** Zeta potential measurements corresponding to different pH (2 to 10) in demi-water.
582 Flocculation zone (gray square) follows Hunter et al. (1981) boundaries. CS 1=Continental Shelf
583 before the mining dam failure; CS 2=Continental Shelf after the failure; RV=River; MD=Mining Dam;
584 PS Goethite = Pure Synthetic Goethite.

585 **Figure 4.** Zeta potential measurements for samples with increasing monovalent salt electrolyte
586 concentrations in demi-water pH = 6.5. The type of electrolyte is indicated to the right of each graph.

589 Shelf before the mining dam failure; CS 2=Continental Shelf after the failure; RV=River; MD=Mining
590 Dam; PS Goethite=Pure Synthetic Goethite.

591 **Figure 5.** Zeta potential measurements for samples with increasing divalent salt electrolyte
592 concentrations in demi-water pH = 6.5. The type of electrolyte is indicated to the right of each graph.
593 Flocculation zone (gray square) with boundaries according to Hunter et al. (1981). Each
594 measurement was made separately for each sample, as indicated in the legend. CS 1=Continental
595 Shelf before the mining dam failure; CS 2=Continental Shelf after the failure; RV=River; MD=Mining
596 Dam; PS Goethite=Pure Synthetic Goethite.

597 **Figure 6**. Zeta potential (mV) as function of PS (Pure Synthetic) goethite addition to CS 1, where CS
598 1=Continental Shelf before the mining dam failure (top panel) and pure kaolinite (bottom panel)
599 suspensions at pH 6.5 (demi-water). The % of goethite indicates the mass percentage of goethite
600 suspension i.e. mass of goethite compared to the clay (kaolinite or CS 1) mass. Flocculation zone
601 (gray square) with boundaries according to Hunter et al. (1981).

602 **Figure 7:** Kaolinite particles (50%) in the presence of goethite (50%) at pH = 3 in demi water; At t = 0
603 (filled square) two zeta potential peaks are observed, one corresponding to kaolinite particles
604 (around -10 mV) and one corresponding to goethite particles (around + 20 mV). After 15 minutes
605 (open square), the particles have aggregated and formed aggregates of zeta potential of
606 approximately 0 mV.

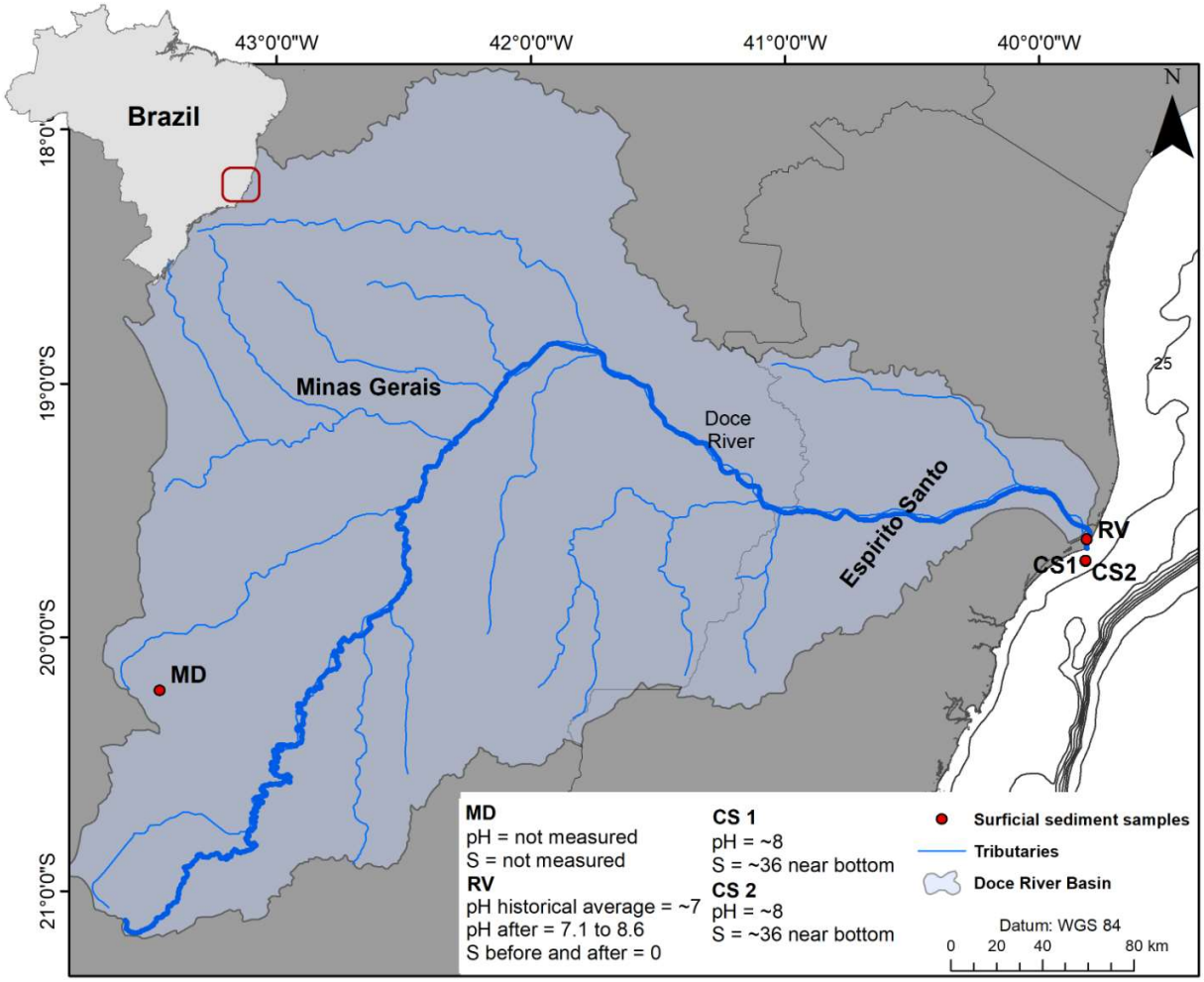

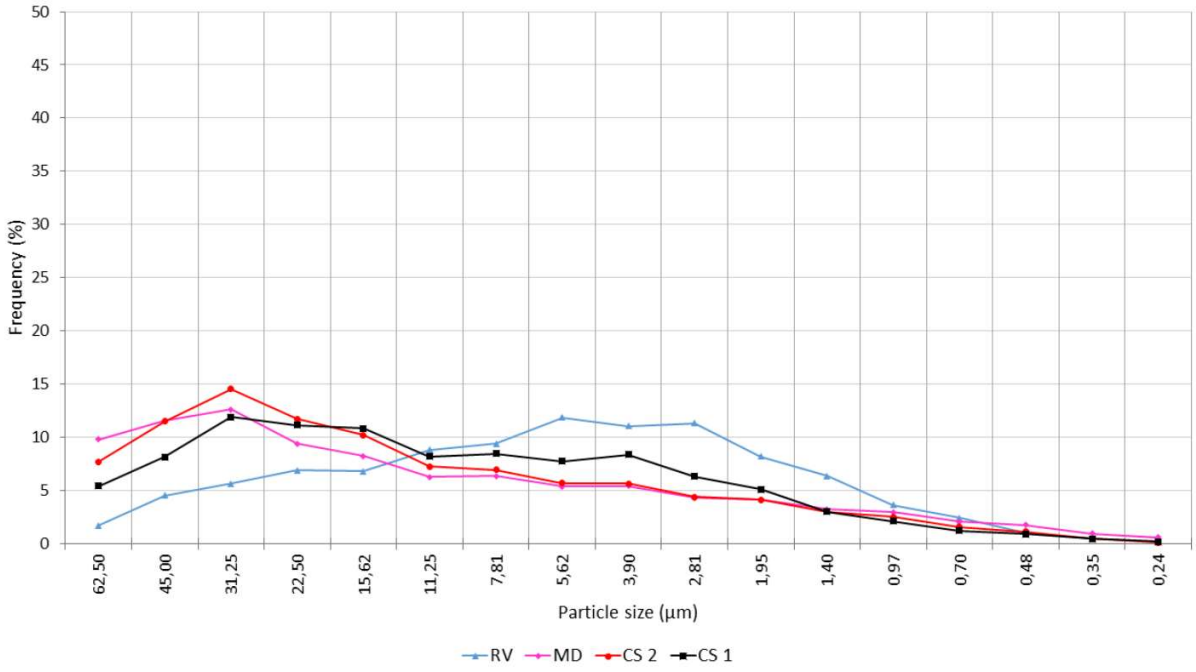

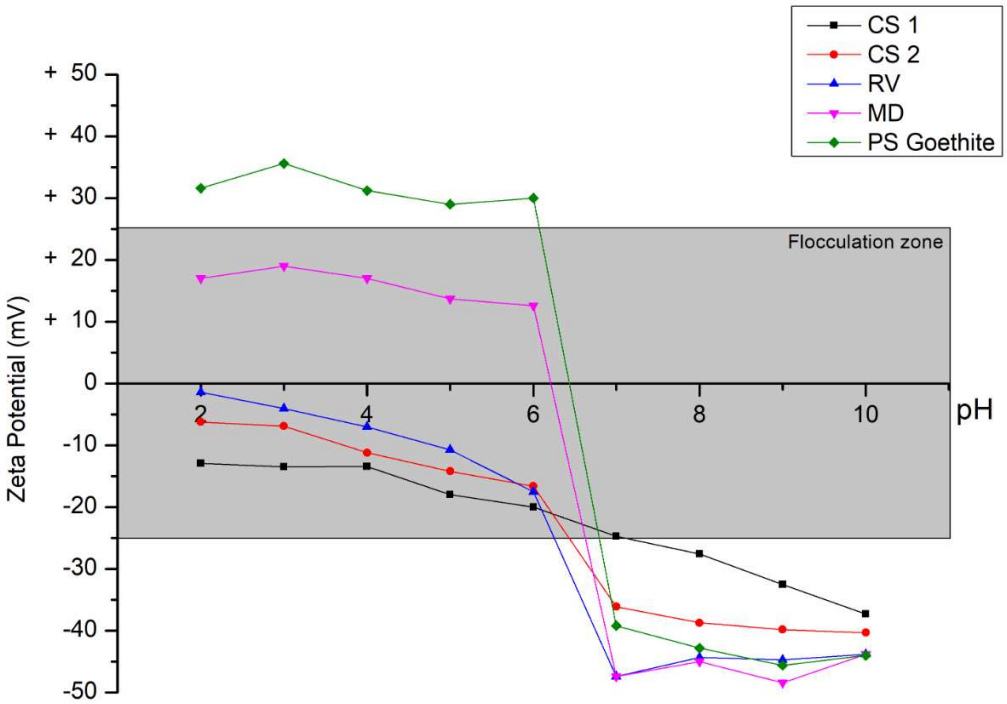

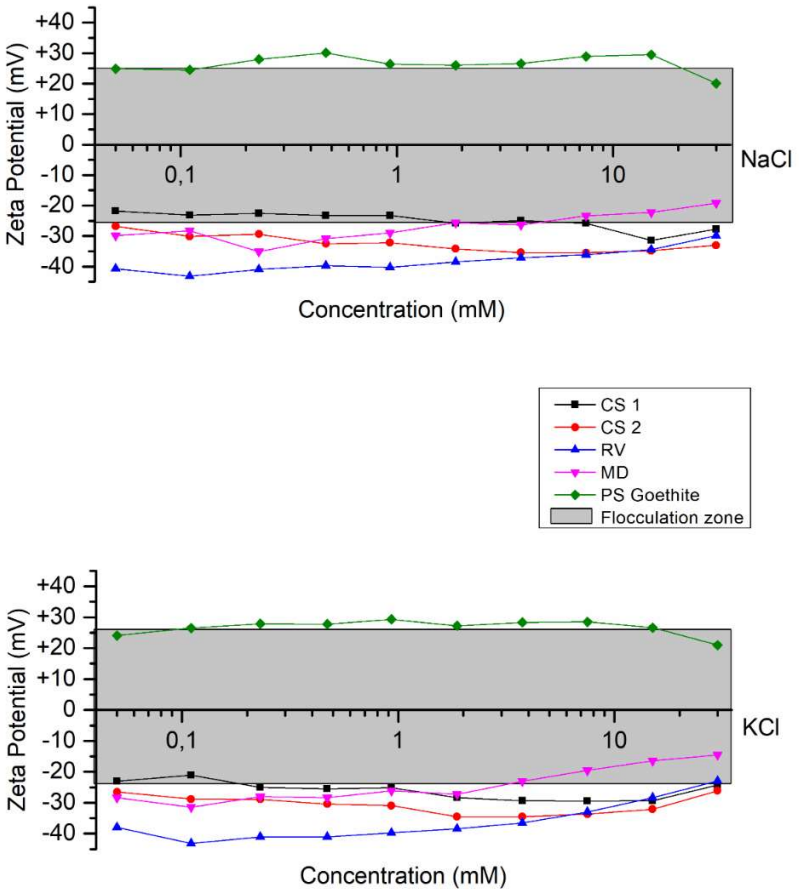

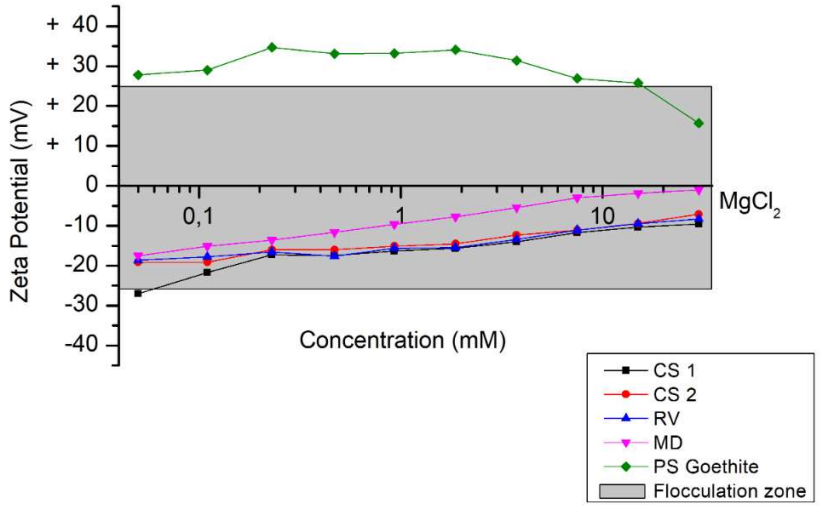

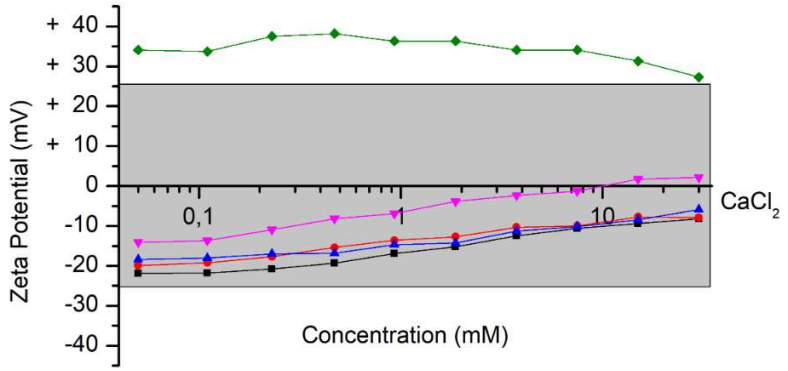

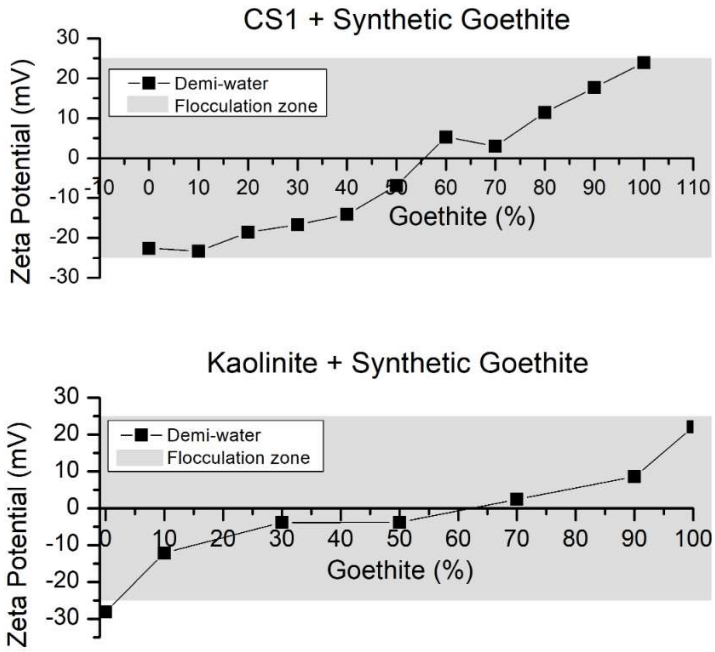

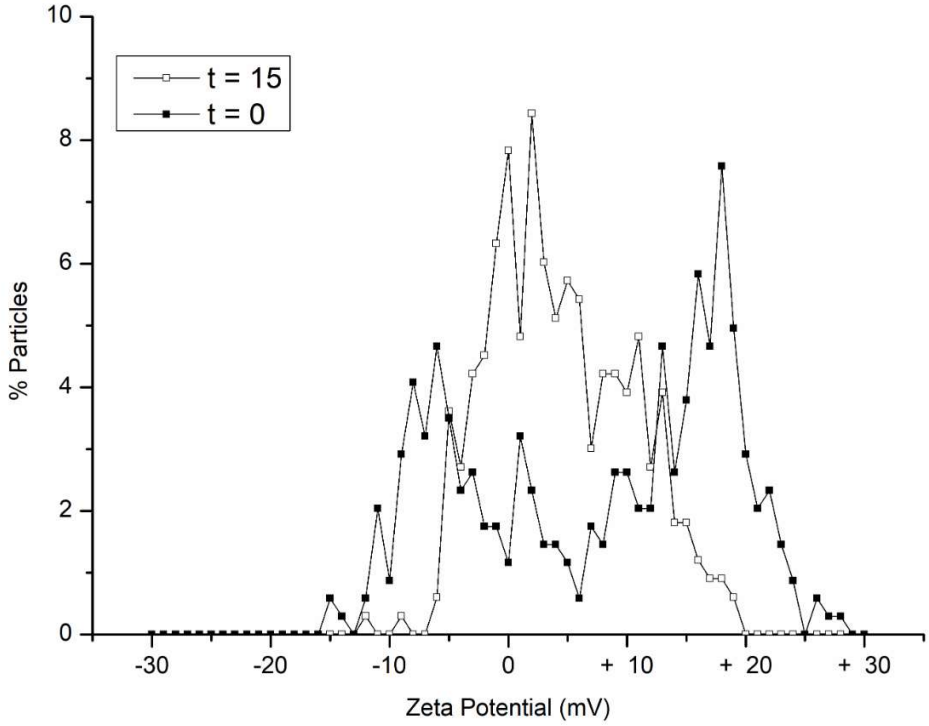

Research highlights

- Material from an iron ore mining dam breach has been exported by the Doce River onto the continental shelf.
- Zeta potential measurements were performed to determine the surface charge of suspended particles in aqueous solution to understand flocculation tendencies.
- Contaminated sediment showed zeta potential behavior similar to goethite while non-contaminated sediment showed a characteristic curve of clay minerals.
- When in marine waters pH, zeta potential had sudden jump in the negative values and left the flocculation tendency zone.
- The amount of tailings in the sediment had a different influence on the behavior of the zeta potential.

All authors reviewed the manuscript. All authors approve submission and publication. All authors declare they have no conflicts of interest.